

# Preparation of hexa-aluminate catalyst thick films on $\alpha$ -SiC substrate for high temperature application

H. INOUE, K. SEKIZAWA, K. EGUCHI, H. ARAI

*Department of Materials Science and Technology, Graduate School of Engineering Sciences, Kyushu University 39, Kasuga, Fukuoka 816, Japan*

The coating of Mn-substituted hexa-aluminate catalysts ( $\text{BaMnAl}_{11}\text{O}_{19-x}$  and  $\text{Sr}_{0.8}\text{La}_{0.2}\text{MnAl}_{11}\text{O}_{19-x}$ ) on  $\alpha$ -SiC substrates was investigated for high temperature application above 1000 °C. The thermal stability of the hexa-aluminate catalyst films on the  $\alpha$ -SiC substrates was significantly affected by reactivity between the oxidized layer ( $\text{SiO}_2$ ) of the surfaces of the substrates and the coated layers. The Mn-substituted hexa-aluminate films were thermally less stable due to their high reactivity than unsubstituted hexa-aluminates. The  $\text{Sr}_{0.8}\text{La}_{0.2}\text{MnAl}_{11}\text{O}_{19-x}$  film directly coated on the substrate exfoliated from the substrate even after heating at 1200 °C due to its high reactivity to the  $\text{SiO}_2$  layer, whereas the  $\text{BaMnAl}_{11}\text{O}_{19-x}$  film was stable after the same treatment. The thermal stability of the Mn-substituted hexa-aluminate film could be improved by insertion of an  $\text{Al}_6\text{Si}_2\text{O}_{13}$  intermediate layer between the film and the SiC substrate. Additional coating of a highly crystallized  $\text{Ba}_{0.75}\text{Al}_{11.0}\text{O}_{17.25}$  intermediate layer underneath the  $\text{BaMnAl}_{11}\text{O}_{19-x}$  catalyst layer was also effective. The  $\text{Al}_6\text{Si}_2\text{O}_{13}$  and  $\text{Ba}_{0.75}\text{Al}_{11.0}\text{O}_{17.25}$  intermediate layers suppressed the diffusion of  $\text{SiO}_2$  from the substrate and subsequent reaction between  $\text{SiO}_2$  and the hexa-aluminate film.

## 1. Introduction

Catalytic combustion has attracted attention as a substitute for conventional flame combustion owing to its many advantages: e.g. high energy efficiency, applicability to lean-fuel combustion, easiness of reaction control and attainability of very low thermal  $\text{NO}_x$  emission [1–3]. In order to apply catalytic combustion to a gas turbine for power supply, which generates a large amount of  $\text{NO}_x$  unless a costly  $\text{deNO}_x$  system is utilized, it is strongly advised to develop both a catalyst material and system to initiate combustion of natural gas from low temperatures and to stabilize the reaction for a long period at  $\sim 1400$  °C. Because such an excellent catalyst material and system have not been well-developed, gas phase combustion has been employed to preheat fuel gas up to the temperature at which catalytic combustion can be initiated and to raise the temperature of the exhaust gas up to the high level of the homogeneous reaction [4, 5].

Hexa-aluminate combustion catalysts reported by our group [6–9] are promising materials with high thermal stability. A typical hexa-aluminate combustion catalyst,  $\text{Sr}_{0.8}\text{La}_{0.2}\text{MnAl}_{11}\text{O}_{19-x}$ , oxidizes 90% of 1 vol %  $\text{CH}_4$  in air at 720 °C. The catalytic activity of the hexa-aluminate for methane combustion is inferior to those of typical noble metal catalysts, such as Pd supported on  $\text{Al}_2\text{O}_3$ , and perovskite-type oxide catalysts. However, high catalytic activities of the Pd or perovskite catalysts are lowered by volatilization of active species and/or sintering of active species, sup-

port and honeycomb body at such high temperatures. Surface areas of hexa-aluminate catalysts are an order of magnitude larger than that of  $\text{Al}_2\text{O}_3$  at about 1400 °C and remain unchanged even after heat treatment at such high temperatures for a long time due to the high sintering resistance. Therefore, hexa-aluminate catalysts have attracted special interest as materials with both high thermal stability and catalytic activity.

The hexa-aluminate catalysts are moulded into a monolithic honeycomb shape by extrusion for practical use [10]. The thermal shock resistance and the mechanical strength of the honeycomb have to be improved, because the catalysts possess relatively large thermal expansion coefficients (about  $8 \times 10^{-6} \text{ K}^{-1}$ ) and have inherent sintering resistances. Furuya *et al.* tried to overcome this problem by segmentation of the hexa-aluminate honeycomb body [11].

The present study aims at preparing a composite catalyst system with a substrate coated with a hexa-aluminate catalyst to improve thermal shock resistance and reliability of the catalyst honeycomb. The material used as the substrate in this study is  $\alpha$ -SiC, which has high thermal shock resistance, thermal stability and mechanical strength.

## 2. Experimental procedure

### 2.1. Preparation of slurry for coating

Two kinds of 12 wt % Mn-substituted hexa-aluminate powders ( $\text{BaMnAl}_{11}\text{O}_{19-x}$  and  $\text{Sr}_{0.8}\text{La}_{0.2}\text{MnAl}_{11}$

$O_{19-\alpha}$ ) were prepared by calcination of hydrolysed precursors. For the preparation of the  $BaMnAl_{11}O_{19-\alpha}$  precursor, calculated amounts of Ba metal and  $Al(OC_3H_7)_3$  were dissolved in 2-propanol and then refluxed at 80 °C in a dry  $N_2$  atmosphere with stirring. After a homogeneous alkoxide solution was obtained, an  $Mn(NO_3)_2$  aqueous solution was pipette dropped and the hydrolysed products were precipitated. To prepare the  $Sr_{0.8}La_{0.2}MnAl_{11}O_{19-\alpha}$  precursor, Sr metal and  $Al(OC_3H_7)_3$  were dissolved in 2-propanol and the resultant alkoxide solution was hydrolysed by pipette dropping an aqueous solution of calculated amounts of  $La(NO_3)_3$  and  $Mn(NO_3)_2$ . The precursors were dried, pyrolysed, calcined at 1200 or 1450 °C, and used as source powders for slurry coating. A slurry of Mn-substituted hexa-aluminate was prepared by adding 12 wt % of the resultant powder to ethanol and subsequent stirring.

To prepare the mullite ( $Al_6Si_2O_{13}$ ) powder, calculated amounts of  $Si(OC_2H_5)_4$  and  $Al(NO_3)_3 \cdot 9H_2O$  were dissolved in absolute ethanol, and the resultant solution was dried and calcined at 1100 °C. Slurries of mullite and commercial  $\gamma-Al_2O_3$ ,  $ZrO_2$  and  $MgO$  powders (6 wt %) were also prepared by mixing with ethanol to investigate reactivity between these ceramic materials and the SiC substrate.

## 2.2. Coating and characterization of films

An  $\alpha$ -SiC substrate was dipped into the slurry and dried at room temperature. The process from dipping to drying was repeated five times. Then, the sample coated with slurry was generally heated at a rate of 200 °C  $h^{-1}$  before keeping the temperature at 1200 °C for 5 h. This sequential coating and heating process was repeated three–five times to develop thick and crack-free films. Some samples were heated at 1300–1500 °C for 5 h in air to check the thermal stability of the film formed. X-ray diffraction (XRD) was carried out to identify the crystalline phase in the film after various treatments. The microstructure of the top and fracture surfaces of the film were observed by a scanning electron microscope (SEM). Elemental analysis of the sample was carried out with an energy-dispersive X-ray (EDX) spectrometer installed on the microscope.

## 3. Results and discussion

### 3.1. Thermal stability of Mn-substituted hexa-aluminate thick films on $\alpha$ -SiC substrate

We have reported the fabrication method of unsubstituted hexa-aluminate ( $Ba_{0.75}Al_{11.0}O_{17.25}$ ) thick film on an  $\alpha$ -SiC substrate and its thermal stability and microstructure [12]. The unsubstituted hexa-aluminate thick film was successfully prepared by slurry coating without the formation of voids. The film attained good adhesion on the smooth oxidized surface of the substrate. The unsubstituted hexa-aluminate film was chemically bonded to the substrate with an intermediate layer consisting of  $BaAl_2Si_2O_8$  and  $\alpha-Al_2O_3$ , which were formed by the reaction between

$SiO_2$  and the hexa-aluminate. The microstructure of the film remained unchanged even after heat treatment at 1300 °C in air. When the heat treatment temperature was raised up to 1400 °C, interfacial reaction was facilitated and the hexa-aluminate film disappeared. The interfacial reaction could be restricted by using highly crystallized powder as a source for the slurry.

Because the unsubstituted hexa-aluminate used for the coating in the previous study is inactive for methane combustion, additional loading of an active material with high thermal stability is needed to complete a catalyst honeycomb system applicable to high temperature combustion. Because substituted Mn ions serve as the redox centre, the Mn-substituted hexa-aluminates exhibit both high catalytic activity for methane combustion and high thermal stability. In this study, two kinds of Mn-substituted hexa-aluminate catalysts ( $BaMnAl_{11}O_{19-\alpha}$  and  $Sr_{0.8}La_{0.2}MnAl_{11}O_{19-\alpha}$ ) were used as active materials.  $Sr_{0.8}La_{0.2}MnAl_{11}O_{19-\alpha}$  has the highest catalytic activity for methane combustion and heat resistance in the series of hexa-aluminate catalysts and thus has been used for a performance test of a prototype catalytic combustor.

Fig. 1a–c shows SEM images of the fracture surfaces of the samples prepared by using slurries with 6 wt %  $Ba_{0.75}Al_{11.0}O_{17.25}$ , 12 wt %  $BaMnAl_{11}O_{19-\alpha}$ , and 12 wt %  $Sr_{0.8}La_{0.2}MnAl_{11}O_{19-\alpha}$ , respectively. The source powders for these slurries were preheated for crystallization at 1100, 1200 and 1300 °C, respectively. Every coated sample was heated at 1200 °C for 5 h in air. An unsubstituted hexa-aluminate ( $Ba_{0.75}Al_{11.0}O_{17.25}$ ) film with a thickness of about 10–20  $\mu m$  was successfully formed and retained up to 1300 °C.

For the samples coated with Mn-substituted hexa-aluminate catalysts, remarkable differences in microstructure were observable. A  $BaMnAl_{11}O_{19-\alpha}$  thick film with a uniform thickness of about 50  $\mu m$  was coated on the SiC substrate. The coated  $Sr_{0.8}La_{0.2}MnAl_{11}O_{19-\alpha}$  film, on the other hand, exfoliated from the substrate. The XRD pattern of this sample indicated that the exfoliated film contained large amounts of  $Al_6Si_2O_{13}$  and  $SrAl_2Si_2O_8$  (Sr-celsian) phases that were formed by reaction between  $SiO_2$  and the hexa-aluminate. This fact is consistent with the reaction model between the film and the substrate as interpreted in our previous report [12]. The observed exfoliation indicates that the heat treatment at 1200 °C in the coating process is higher than the limit of thermal stability of the  $Sr_{0.8}La_{0.2}MnAl_{11}O_{19-\alpha}$  film. The upper limit for the heat treatment is strongly dependent on the reactivity between  $SiO_2$  on the surface of the substrate and the film. Accordingly, the differences in stabilities of coated  $BaMnAl_{11}O_{19-\alpha}$  or  $Sr_{0.8}La_{0.2}MnAl_{11}O_{19-\alpha}$  result from the formation rates of  $BaAl_2Si_2O_8$  and  $SrAl_2Si_2O_8$ . It is, therefore, concluded that Ba-based hexa-aluminate thick film is thermally more stable on  $\alpha$ -SiC substrate than Sr-based hexa-aluminate.

The thermal stability of the  $BaMnAl_{11}O_{19-\alpha}$  thick film on the substrate was evaluated from a backscattered

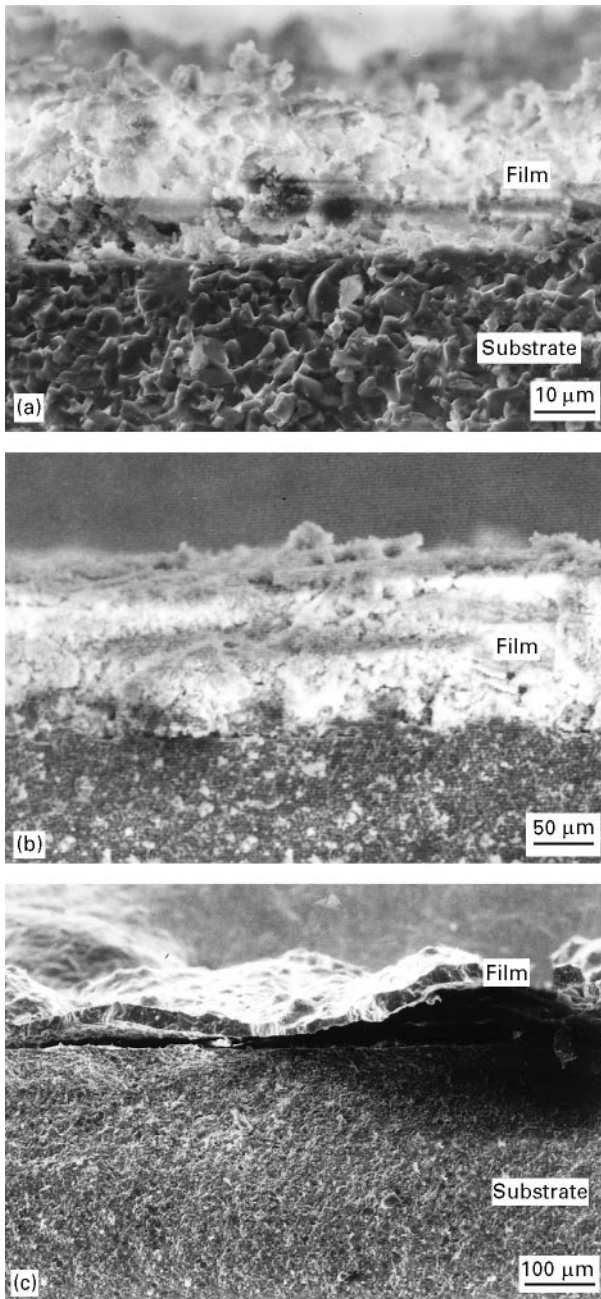


Figure 1 SEM images of the fracture surfaces of (a)  $\text{Ba}_{0.75}\text{Al}_{11.0}\text{O}_{17.25}$ , (b)  $\text{BaMnAl}_{11}\text{O}_{19-\alpha}$ , and (c)  $\text{Sr}_{0.8}\text{La}_{0.2}\text{MnAl}_{11}\text{O}_{19-\alpha}$  films prepared on  $\alpha$ -SiC substrates by slurry coating and subsequently heated at 1200 °C for 5 h in air.

electron image of the fracture surface of the sample after heat treatment at 1300 °C for 5 h in air (Fig. 2). Although a film about 50  $\mu\text{m}$  in thickness remained on the substrate, its microstructure was extremely different from that before heat treatment. The formation of voids at the interface between the substrate and the film indicated that a significant extent of reaction proceeded. The crystalline phases identified were  $\alpha$ - $\text{Al}_2\text{O}_3$  and  $\text{BaAl}_2\text{Si}_2\text{O}_8$ , but the  $\text{BaMnAl}_{11}\text{O}_{19-\alpha}$  phase disappeared. EDX analysis indicated that  $\text{SiO}_2$ ,  $\text{BaAl}_2\text{Si}_2\text{O}_8$ , or  $\alpha$ - $\text{Al}_2\text{O}_3$  were the dominant components in the grey, white or black parts of the image. It is apparent that  $\text{SiO}_2$  exists even in the topmost part of the film. The poor thermal stability of the  $\text{BaMnAl}_{11}\text{O}_{19-\alpha}$  film suggests that Mn facilitates the reaction between  $\text{SiO}_2$  and the hexa-aluminate phase and the formation of  $\text{BaAl}_2\text{Si}_2\text{O}_8$ .

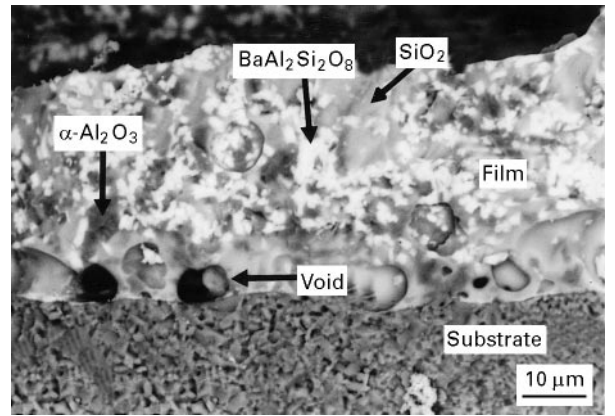


Figure 2 Backscattered electron image of the fracture surface of the  $\text{BaMnAl}_{11}\text{O}_{19-\alpha}$  film after heat treatment at 1300 °C.

### 3.2. Effect of buffer layers on the thermal stability of Mn-substituted hexa-aluminate thick film

In order to improve the thermal stability of hexa-aluminate films on an  $\alpha$ -SiC substrates, it is necessary to avoid direct contact and resultant reaction between  $\text{SiO}_2$  and hexa-aluminates, because the reaction is obviously facilitated by Mn. Insertion of some ceramic layers ( $\text{ZrO}_2$ ,  $\text{Al}_6\text{Si}_2\text{O}_{13}$ ,  $\text{Al}_2\text{O}_3$  and  $\text{MgO}$ ) between the substrates and the hexa-aluminate layers was investigated in this study. The reactivities between the  $\alpha$ -SiC substrates and these ceramic materials were evaluated from the SEM images after coating on the SiC substrates and subsequent heating at 1500 °C for 5 h in air (Fig. 3). The sample coated with  $\text{Al}_2\text{O}_3$  contained an  $\text{Al}_6\text{Si}_2\text{O}_{13}$  phase and large voids at the interface between the substrate and the film. The  $\text{MgO}$  film exfoliated from the substrate. On the other hand, the samples coated with  $\text{ZrO}_2$  or  $\text{Al}_6\text{Si}_2\text{O}_{13}$  formed glassy phase  $\text{SiO}_2$  even at the top surface. But exfoliation was hardly observable. In the case of the  $\text{ZrO}_2$  film,  $\text{ZrSiO}_4$  formed as a minority phase by reaction with  $\text{SiO}_2$ . In the case of the  $\text{Al}_6\text{Si}_2\text{O}_{13}$  film, no reaction product was formed. From these results,  $\text{ZrO}_2$  and  $\text{Al}_6\text{Si}_2\text{O}_{13}$  films were selected as the intermediate layers. It is suggested that  $\text{ZrO}_2$  exists stably on the substrate because of the slow formation rate of  $\text{ZrSiO}_4$ . Because mixed phases of  $\text{Al}_6\text{Si}_2\text{O}_{13}$  and  $\text{SiO}_2$  are in equilibrium in the composition range  $\text{Al}/\text{Si} < 3$  from the  $\text{SiO}_2$ - $\text{Al}_2\text{O}_3$  phase diagram [13], the  $\text{Al}_6\text{Si}_2\text{O}_{13}$  film is stable on the substrate without reacting with  $\text{SiO}_2$ .

Backscattered electron images of the fracture surfaces of the samples with the  $\text{ZrO}_2$  intermediate layer between the substrate and the  $\text{Sr}_{0.8}\text{La}_{0.2}\text{MnAl}_{11}\text{O}_{19-\alpha}$  film after heat treatment at 1200 and 1300 °C for 5 h in air after the coating process are shown in Fig. 4a and b, respectively. As described above, when  $\text{Sr}_{0.8}\text{La}_{0.2}\text{MnAl}_{11}\text{O}_{19-\alpha}$  was coated directly on the substrate, the film exfoliated after heat treatment at 1200 °C. On the other hand, the hexa-aluminate thick films (about 50  $\mu\text{m}$  thick) were successfully prepared on the intermediate layer. The XRD patterns of the samples are shown in Fig. 5a and b. The XRD lines for the sample heat treated at 1200 °C were assigned to  $\text{ZrSiO}_4$ ,

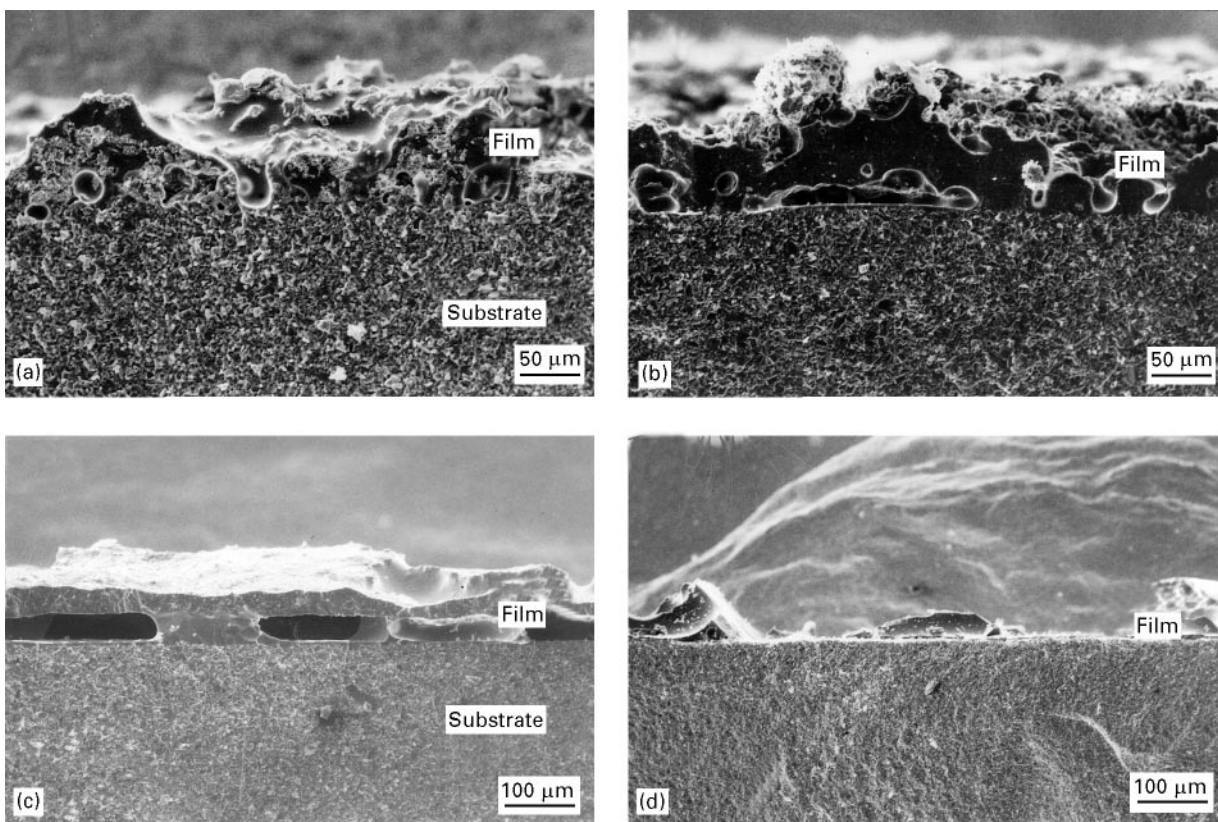


Figure 3 SEM images of the fracture surfaces of (a)  $\text{ZrO}_2$ , (b)  $\text{Al}_6\text{Si}_2\text{O}_{13}$ , (c)  $\text{Al}_2\text{O}_3$ , and (d)  $\text{MgO}$  films coated on  $\alpha\text{-SiC}$  substrates. Every sample was heated at  $1500^\circ\text{C}$  for 5 h in air.

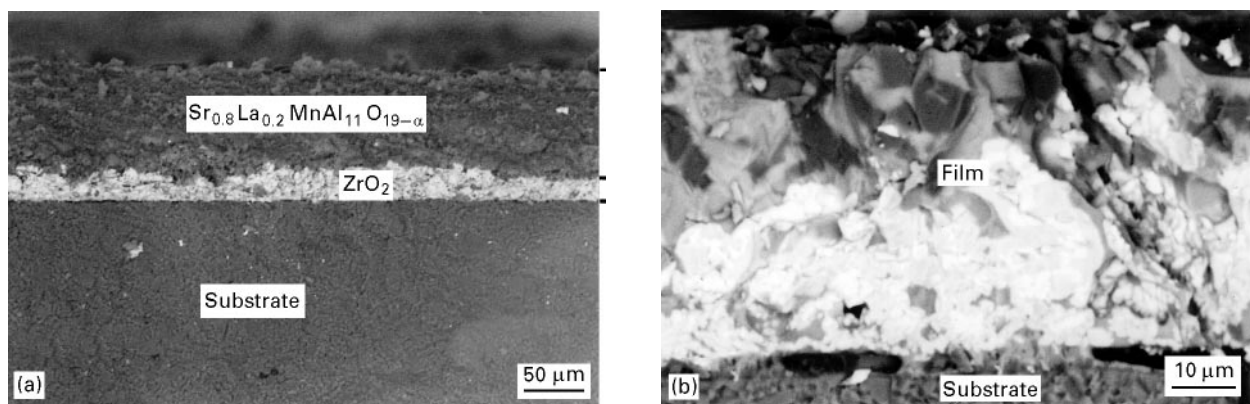


Figure 4 Backscattered electron images of the fracture surfaces of samples with  $\text{ZrO}_2$  intermediate and  $\text{Sr}_{0.8}\text{La}_{0.2}\text{MnAl}_{11}\text{O}_{19-\alpha}$  topmost layers after heat treatment at (a)  $1200^\circ\text{C}$  and (b)  $1300^\circ\text{C}$ .

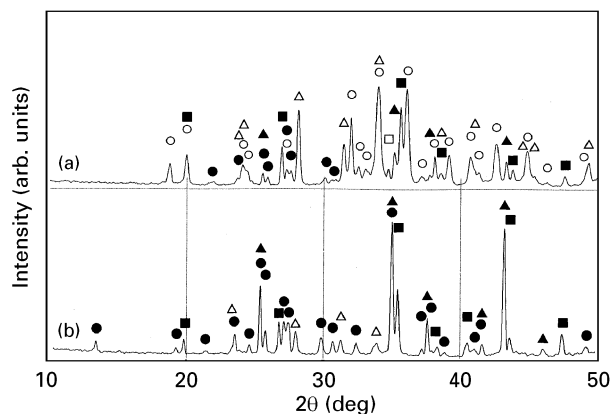


Figure 5 XRD patterns of samples with  $\text{ZrO}_2$  intermediate and  $\text{Sr}_{0.8}\text{La}_{0.2}\text{MnAl}_{11}\text{O}_{19-\alpha}$  topmost layers after heat treatment at (a)  $1200^\circ\text{C}$  and (b)  $1300^\circ\text{C}$ . (○)  $\text{SrAl}_{12}\text{O}_{19}$ , (●)  $\text{SrAl}_2\text{Si}_2\text{O}_8$ , (△)  $\text{ZrO}_2$ , (▲)  $\alpha\text{-Al}_2\text{O}_3$ , (■)  $\text{ZrSiO}_4$ , (□) unknown.

$\text{ZrO}_2$ ,  $\text{SrAl}_2\text{Si}_2\text{O}_8$  and  $\alpha\text{-Al}_2\text{O}_3$  in addition to the Sr-hexa-aluminate phase. The  $\text{SiO}_2$  species migrated to the topmost part of the  $\text{ZrO}_2$  intermediate layer even at  $1200^\circ\text{C}$  and reacted with the hexa-aluminate layer. After heating at  $1300^\circ\text{C}$ , peaks from the hexa-aluminate phase disappeared completely and those from  $\text{SrAl}_2\text{Si}_2\text{O}_8$  and  $\alpha\text{-Al}_2\text{O}_3$  phases intensified. Fig. 6a and b shows XRD patterns of the samples with  $\text{Al}_6\text{Si}_2\text{O}_{13}$  intermediate and  $\text{Sr}_{0.8}\text{La}_{0.2}\text{MnAl}_{11}\text{O}_{19-\alpha}$  topmost layers after heat treatment at  $1200^\circ\text{C}$  and  $1300^\circ\text{C}$  for 5 h in air, respectively. Only the Sr-hexa-aluminate phase appeared in the XRD pattern of the sample heat treated at  $1200^\circ\text{C}$ . Therefore, the  $\text{Al}_6\text{Si}_2\text{O}_{13}$  layer is less reactive to  $\text{SiO}_2$  than the  $\text{ZrO}_2$  layer. Although the reaction products also formed with increasing heat treatment temperature to  $1300^\circ\text{C}$ , the hexa-aluminate phase still remained on

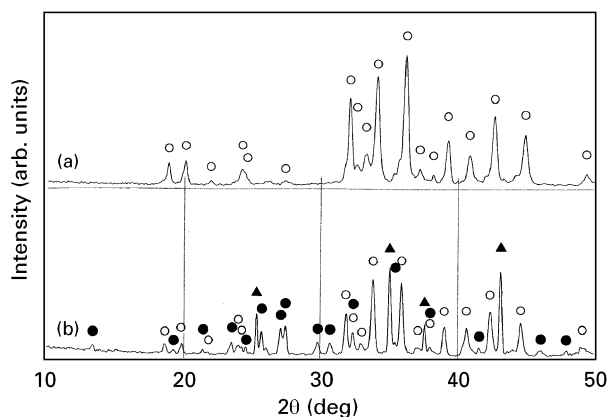


Figure 6 XRD patterns of samples with  $\text{Al}_6\text{Si}_2\text{O}_{13}$  intermediate and  $\text{Sr}_{0.8}\text{La}_{0.2}\text{MnAl}_{11}\text{O}_{19-x}$  topmost layers after heat treatment at (a) 1200 and (b) 1300 °C. (○)  $\text{SrAl}_{12}\text{O}_{19}$ , (●)  $\text{SrAl}_2\text{Si}_2\text{O}_8$ , (▲)  $\alpha\text{-Al}_2\text{O}_3$ .

the  $\text{Al}_6\text{Si}_2\text{O}_{13}$  intermediate layer. SEM backscattered images of the fracture surfaces of the samples are shown in Fig. 7a and b. The microstructure of the fine-grained thick film heat treated at 1300 °C re-

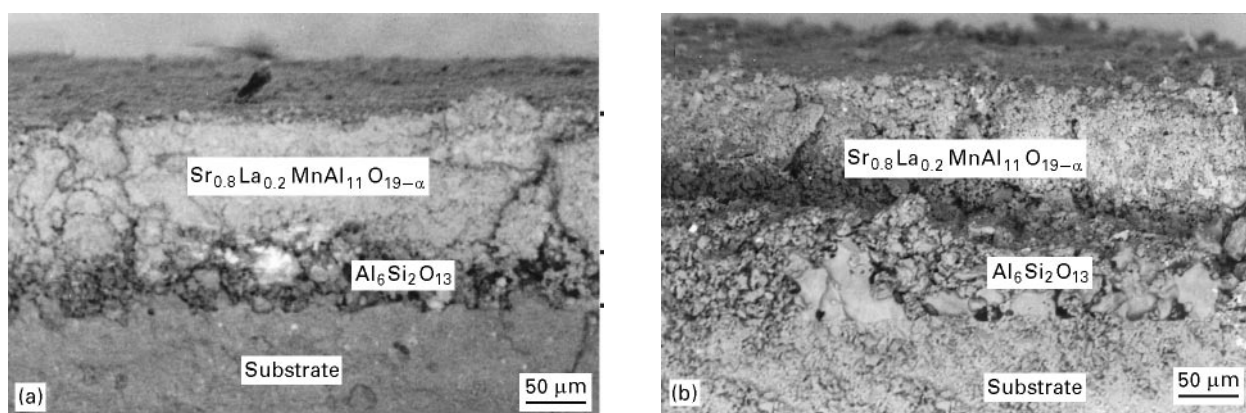


Figure 7 Backscattered electron images of fracture surfaces of samples with  $\text{Al}_6\text{Si}_2\text{O}_{13}$  intermediate and  $\text{Sr}_{0.8}\text{La}_{0.2}\text{MnAl}_{11}\text{O}_{19-x}$  topmost layers after heat treatment at (a) 1200 and (b) 1300 °C.

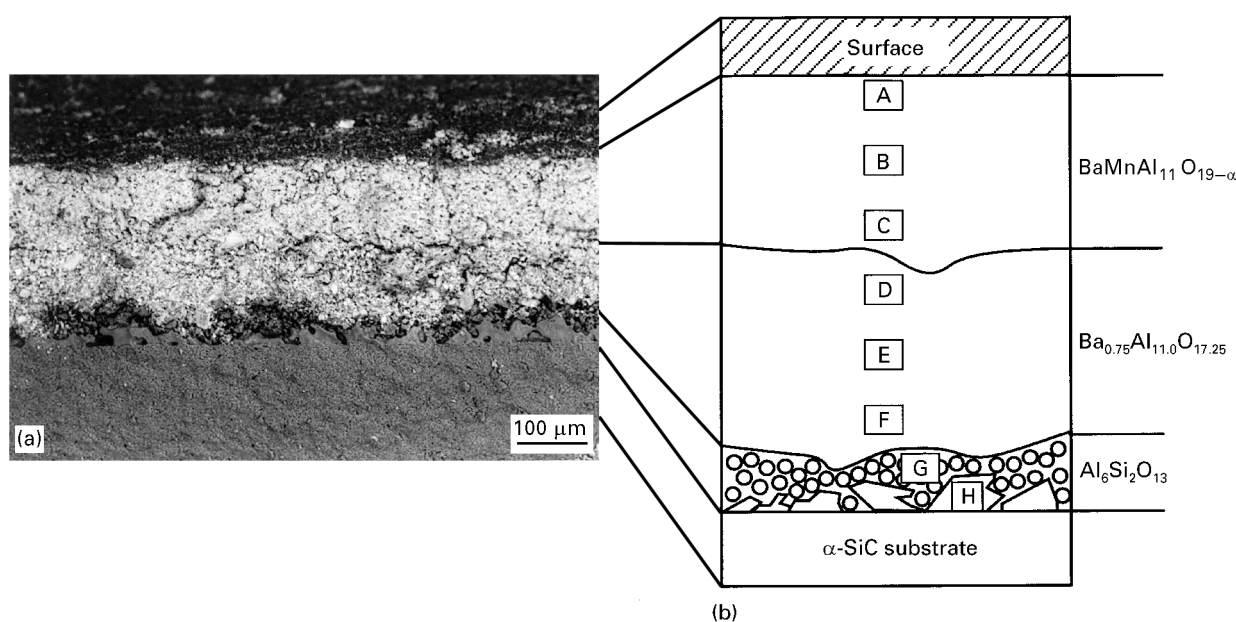


Figure 8 (a) Backscattered electron image and (b) a schematic illustration of the fracture surface of the quadruple layered sample of  $\text{BaMnAl}_{11}\text{O}_{19-x}/\text{Ba}_{0.75}\text{Al}_{11.0}\text{O}_{17.25}/\text{Al}_6\text{Si}_2\text{O}_{13}/\alpha\text{-SiC}$  after heat treatment at 1400 °C for 5 h in air. Source powders for hexa-aluminate slurries were calcined at 1450 °C for 5 h in air.

maintained almost unchanged as compared with that after heat treatment at 1200 °C. Large glassy particles were formed in the intermediate layer after heat treatment at 1300 °C, which appeared to be formed by reaction with  $\text{SiO}_2$ . Thus, the  $\text{Al}_6\text{Si}_2\text{O}_{13}$  intermediate layer was effective in suppressing interlayer diffusion of  $\text{SiO}_2$  and, consequently, the  $\text{Sr}_{0.8}\text{La}_{0.2}\text{MnAl}_{11}\text{O}_{19-x}$  film was maintained even after heating at 1300 °C.

Even in the  $\text{Sr}_{0.8}\text{La}_{0.2}\text{MnAl}_{11}\text{O}_{19-x}-\text{Al}_6\text{Si}_2\text{O}_{13}-\text{SiC}$  triple layer, solid state reaction between the  $\text{Sr}_{0.8}\text{La}_{0.2}\text{MnAl}_{11}\text{O}_{19-x}$  film and  $\text{SiO}_2$  occurred at the  $\text{Sr}_{0.8}\text{La}_{0.2}\text{MnAl}_{11}\text{O}_{19-x}-\text{Al}_6\text{Si}_2\text{O}_{13}$  interface at 1300 °C, as shown in Fig. 6b. Accordingly, a further increase in heat treatment temperature led to the disappearance of the hexa-aluminate film. Therefore, the following conditions are considered to be efficient:

1. Choose  $\text{BaMnAl}_{11}\text{O}_{19-x}$ , which is less reactive to  $\text{SiO}_2$  than  $\text{Sr}_{0.8}\text{La}_{0.2}\text{MnAl}_{11}\text{O}_{19-x}$ , as the coated catalyst layer.
2. Insert a  $\text{Ba}_{0.75}\text{Al}_{11.0}\text{O}_{17.25}$  layer between  $\text{Al}_6\text{Si}_2\text{O}_{13}$  and the Mn-substituted hexa-aluminate film as the second intermediate layer.

TABLE I Local content of Mn and Si in BaMnAl<sub>11</sub>O<sub>19-α</sub>/Ba<sub>0.75</sub>Al<sub>11.0</sub>O<sub>17.25</sub>/Al<sub>6</sub>Si<sub>2</sub>O<sub>13</sub> film<sup>a</sup> after heat treatment at 1400 °C for 5 h in air

Position	Content (at %)	
	Mn	Si
A	7.13	1.50
B	7.88	0.73
C	9.50	0.39
D	4.09	6.85
E	5.01	2.26
F	3.90	3.26
G	0.18	30.67
H	2.04	54.61

<sup>a</sup>Source powders for hexa-aluminate slurries were calcined at 1450 °C for 5 h in air.

3. Use highly crystallized powders as the source powders for the slurry, as has been suggested in a previous report [12].

From these points of view, a quadruple layered sample of BaMnAl<sub>11</sub>O<sub>19-α</sub>-Ba<sub>0.75</sub>Al<sub>11.0</sub>O<sub>17.25</sub>-Al<sub>6</sub>Si<sub>2</sub>O<sub>13</sub>-SiC was built up by coating with highly crystallized hexa-aluminate powders calcined at 1450 °C for 5 h and subsequently heat treated at 1400 °C for 5 h in air. A backscattered electron image of the fracture surface is shown in Fig. 8, together with its schematic phase distribution. The local contents of Mn and Si in the film formed were analysed by EDX (Table I). Small cracks parallel to the surface of the substrate can be seen in the central parts of the hexa-aluminate film. Judging from the coating processes and the film thickness, these cracks were generated at the interface between the BaMnAl<sub>11</sub>O<sub>19-α</sub> and Ba<sub>0.75</sub>Al<sub>11.0</sub>O<sub>17.25</sub> films. The fine microstructures of both hexa-aluminate films were maintained even after the heat treatment at 1400 °C and thus extremely high thermal stability of this layered sample was obvious. The result of the EDX analysis indicated that large grains formed in the Al<sub>6</sub>Si<sub>2</sub>O<sub>13</sub> layer (position H) have a very high Si content and a relatively large amount of Mn species diffused into Ba<sub>0.75</sub>Al<sub>11.0</sub>O<sub>17.25</sub> film. The Al<sub>6</sub>Si<sub>2</sub>O<sub>13</sub> and Ba<sub>0.75</sub>Al<sub>11.0</sub>O<sub>17.25</sub> intermediate layers effectively suppress the diffusion of SiO<sub>2</sub> from the substrate and the reaction between SiO<sub>2</sub> and the hexa-aluminate film, respectively. It is important to locate the Mn component separately away from the Si component. The high crystallinities of the BaMnAl<sub>11</sub>O<sub>19-α</sub> and Ba<sub>0.75</sub>Al<sub>11.0</sub>O<sub>17.25</sub> powders were also effective in suppressing the solid state reactions.

#### 4. Conclusions

The thermal stability of hexa-aluminate films coated on an α-SiC substrate depended on the reactivity between the SiO<sub>2</sub> and the hexa-aluminates. Because Mn facilitated the reactions, Mn-substituted hexa-aluminate films were thermally less stable than the unsubstituted films. Although the

Sr<sub>0.8</sub>La<sub>0.2</sub>MnAl<sub>11</sub>O<sub>19-α</sub> film exfoliated from the substrate even after heat treatment at 1200 °C, the BaMnAl<sub>11</sub>O<sub>19-α</sub> film formed successfully after the same heat treatment. This difference in thermal stability was suggested to result from ease in formation of SrAl<sub>2</sub>Si<sub>2</sub>O<sub>8</sub>.

The Sr<sub>0.8</sub>La<sub>0.2</sub>MnAl<sub>11</sub>O<sub>19-α</sub> films with about 50 μm thickness were successfully formed on the ZrO<sub>2</sub> or Al<sub>6</sub>Si<sub>2</sub>O<sub>13</sub> intermediate layer after heat treatment at 1200 °C. Because the Al<sub>6</sub>Si<sub>2</sub>O<sub>13</sub> intermediate layer was more effective in suppressing interlayer diffusion of SiO<sub>2</sub>, the Sr<sub>0.8</sub>La<sub>0.2</sub>MnAl<sub>11</sub>O<sub>19-α</sub> film was maintained even after heating at 1300 °C. The quadruple layered sample of BaMnAl<sub>11</sub>O<sub>19-α</sub>-Ba<sub>0.75</sub>Al<sub>11.0</sub>O<sub>17.25</sub>-Al<sub>6</sub>Si<sub>2</sub>O<sub>13</sub>-SiC had extremely high thermal stability up to 1400 °C. The Al<sub>6</sub>Si<sub>2</sub>O<sub>13</sub> and Ba<sub>0.75</sub>Al<sub>11.0</sub>O<sub>17.25</sub> intermediate layers effectively suppressed the diffusion of SiO<sub>2</sub> from the substrate and the reaction between SiO<sub>2</sub> and the hexa-aluminate film, respectively. The high crystallinities of these hexa-aluminate powders were also effective in suppressing the solid state reactions.

#### Acknowledgements

The present work was partially supported by the Grant-in-Aid for Science Research from the Ministry of Education, Japan.

#### References

1. D. L. TRIMM, *Appl. Catal.* **7** (1983) 249.
2. L. D. PFEFFERLE and W. C. PFEFFERLE, *Catal. Rev. Sci. Eng.* **29** (2&3) (1987) 219.
3. M. F. M. ZWINKELS, S. G. JÄRÅS, P. G. MENON and T. A. GRIFFIN, *ibid.* **35** (1993) 319.
4. T. FURUYA, T. HAYATA, S. YAMANAKA, J. KOEZUKA, T. YOSHINE and A. OKOSHI, Paper 87-GT-9 (American Society for Mechanical Engineers, Boston, MA, 1987).
5. T. FURUYA, K. SASAKI, Y. HANAKATA, K. MITSUYASU, M. YAMADA, T. TSUCHIYA, and Y. FURUSE, in Proceedings of the International Workshop on Catalytic Combustion, Tokyo, April 1994, edited by H. Arai (Catalysis Society of Japan, Tokyo, 1994) p. 162.
6. M. MACHIDA, K. EGUCHI and H. ARAI, *Chem. Lett.* **1987** (1987) 767.
7. M. MACHIDA, K. KAWASAKI, K. EGUCHI and H. ARAI, *ibid.* **1988** (1987) 1461.
8. M. MACHIDA, K. EGUCHI and H. ARAI, *J. Catal.* **120** (1989) 377.
9. *Idem, ibid.* **123** (1990) 477.
10. H. SADAMORI, T. TANIOKA and T. MATSUHISA, in Proceedings of the International Workshop on Catalytic Combustion, Tokyo, April 1994, edited by H. Arai (Catalysis Society of Japan, Tokyo, 1994) p. 158.
11. A. FURUYA, T. NISHIDA and T. MATSUHISA, *ibid.* p. 70.
12. H. INOUE, K. SEKIZAWA, K. EGUCHI and H. ARAI, *J. Amer. Ceram. Soc.* **80** (1997) 584.
13. R. S. ROTH, J. R. DENNIS and H. F. McMURDIE, "Phase diagrams for ceramists", Vol. VI (The American Ceramic Society, Westerville, 1987) p. 146.

Received 7 March 1996  
and accepted 26 February 1997